

Metal-doped magic clusters of Si, Ge, and Sn: The finding of a magnetic superatom

Vijay Kumar and Yoshiyuki Kawazoe

Citation: *Appl. Phys. Lett.* **83**, 2677 (2003); doi: 10.1063/1.1609661

View online: <http://dx.doi.org/10.1063/1.1609661>

View Table of Contents: <http://apl.aip.org/resource/1/APPLAB/v83/i13>

Published by the [American Institute of Physics](http://www.aip.org).

Related Articles

Electronic and vibrational properties of vanadium-carbide nanowires

J. Appl. Phys. **112**, 063502 (2012)

Theoretical investigation of the electronic structures and carrier transport of hybrid graphene and boron nitride nanostructure

AIP Advances **2**, 032133 (2012)

Methods for fast evaluation of self-energy matrices in tight-binding modeling of electron transport systems

J. Appl. Phys. **112**, 013711 (2012)

Electronic structures of zigzag SiC nanoribbons with asymmetric hydrogen-terminations

Appl. Phys. Lett. **101**, 013102 (2012)

Surface effect on electronic and optical properties of Bi₂Ti₂O₇ nanowires for visible light photocatalysis

J. Appl. Phys. **111**, 124306 (2012)

Additional information on *Appl. Phys. Lett.*

Journal Homepage: <http://apl.aip.org/>

Journal Information: http://apl.aip.org/about/about_the_journal

Top downloads: http://apl.aip.org/features/most_downloaded

Information for Authors: <http://apl.aip.org/authors>

ADVERTISEMENT



Goodfellow
metals • ceramics • polymers • composites
70,000 products
450 different materials
small quantities fast

www.goodfellowusa.com

Metal-doped magic clusters of Si, Ge, and Sn: The finding of a magnetic superatom

Vijay Kumar^{a)} and Yoshiyuki Kawazoe

Institute for Materials Research, Tohoku University, 2-1-1 Katahira Aoba-ku, Sendai 980-8577, Japan

(Received 7 May 2002; accepted 16 July 2003)

Studies on divalent-metal (M)-atom-doped $X_N M$ ($X = \text{Si, Ge, and Sn}$, $N = 8-12$ and 14) clusters, using *ab initio* pseudopotential plane wave method, show that the well known nine- and ten-atom capped prism units as well as 12- and 14-atom clusters of these elements can transform to magic clusters with higher symmetries and larger highest occupied–lowest unoccupied molecular orbital gaps. Most strikingly doping of X_{12} with Mn leads to an icosahedral superatom, $\text{Mn}@X_{12}$, $X = \text{Ge and Sn}$ with a high magnetic moment of $5 \mu_B$, enriching the family of M -doped clusters of semiconductors for possible nanodevice applications. © 2003 American Institute of Physics.
[DOI: 10.1063/1.1609661]

Recent findings^{1–3} of caged clusters of Si by M encapsulation have generated much excitement in exploring clusters for nanodevices. The size and properties of such clusters can be manipulated by choosing an M atom that also enhances the stability of the X cages and could give rise to clusters with high symmetries^{1,4,5} as well as large (HOMO–LUMO) gaps for applications in optoelectronic devices. This is in contrast to X_N clusters with $N = 12-16$ that are not too abundant and have low symmetries.⁶ Most interestingly, it could be possible to produce such clusters with remarkable size selection. In a striking result, perfect icosahedral (i) clusters of Ge and Sn with large HOMO–LUMO gaps of ≈ 2 eV, were obtained⁵ by divalent M doping. The relative sizes of the M atom and the X cage are important for their stability. Here we study doping of different divalent M atoms and report the finding of Mn doped i clusters of Ge and Sn with $5 \mu_B$ magnetic moment in accordance with the Hund's rule in clusters.⁷ Also doping of X_9 and X_{10} leads to new magic clusters while $M@X_{14}$ is a *superatom* with perfect body centered cubic (c) structure.

The calculations have been done for $N = 8-12$ and 14 using *ab initio* ultrasoft pseudopotential plane wave method⁸ and spin-polarized generalized gradient approximation⁹ (GGA) for the exchange-correlation energy. A simple cubic supercell of size up to 20 \AA is used with periodic boundary conditions and the Γ point, for the Brillouin zone integrations. For charged clusters a neutralizing uniform background is used. A few selected structures are optimized using the conjugate gradient method without any symmetry constraint to explore the lowest energy structures. For M we consider Be, Zn, Cd, and Mg and treat the d electrons also as valence for Sn, Zn, and Cd. Mn is considered as a special case as it also behaves like a divalent M atom with a half filled $3d$ level and $4s^2$ closed shell electronic configuration. The converged structures have zero spin in all cases except for Mn doping. The dynamic stability of clusters is studied

using the Gaussian method with $6-311+G^*$ basis set within GGA.¹⁰

The low lying isomers are shown in Fig. 1 and the doping energy (DE) of M in X_N , defined as the difference in energy of the ground state of X_N plus the M atom minus the energy of the doped cluster, in Fig. 2. For $N = 8$, a nearly regular c structure [Fig. 1(a)] is stable in most cases with a large HOMO–LUMO gap¹¹ (Table I). A capped pentagonal bipyramid (PBP) relaxes significantly [Fig. 1(b)] and is nearly degenerate with a smaller gap (Table I). The DE is highest for $M = \text{Be}$ and it decreases as the size of the M atom increases. The DE of Be increases from $X = \text{Si}$ to Ge but then decreases for Sn due to its large size so that Be is not optimally bonded (Fig. 2). On the other hand for Zn, the DE is highest for $X = \text{Sn}$ as it is compressed in Si and Ge cages. For Cd it is often more favorable to place the dopant outside X_N due to its large size. Calculations on $X_9 M$ show it to be more stable than $X_8 M$ in all cases (Fig. 2). Its structure is obtained by doping an M atom at the center of a tricapped prism. After optimization a triangular face opens up a little and the M atom either remains inside as in Be doped clusters [Fig. 1(c)] or comes out almost in the plane of this triangle as in Ge_9Zn and Sn_9Cd or outside as in the case of Ge_9Cd with a structure similar to Ge_{10} . An interesting behavior is found for Si_9Zn which has two nearly degenerate configurations of Zn outside the triangle but a large difference in the gap: (i) close to the plane of the triangle [Fig. 1(d)] with a gap of 1.59 eV and (ii) slightly away from the triangle [Fig. 1(e)] as Si_{10} with a gap of 0.78 and 0.02 eV lower energy than the former. The gap and the binding energy (BE), defined with respect to free atoms, of Si_9Be increase to 1.93 and 3.72 eV/atom as compared to 1.59 and 3.69 eV/atom, respectively, for Si_9 , making the former more stable.

Studies of $M@X_{10}$ in the c (bicapping of a cube on opposite faces) and tetracapped prism structures show the latter to be slightly lower in energy. It transforms to a higher symmetry D_{4d} structure [Fig. 1(f)]. The HOMO–LUMO gap of $\text{Be}@X_{10}$ is 1.68 eV as compared to 2.09 eV for Si_{10} . However, the DE (3.42 eV) is more than 3.0 eV obtained by adding a Si atom to Si_{10} , making $\text{Be}@X_{10}$ more favorable.

^{a)}Also at: Center for Interdisciplinary Research, Tohoku University, Sendai 980-8578, Japan and Dr. Vijay Kumar Foundation, 45 Bazaar St., K.K. Nagar (West), Chennai 600 078, India; electronic mail: kumar@imr.edu

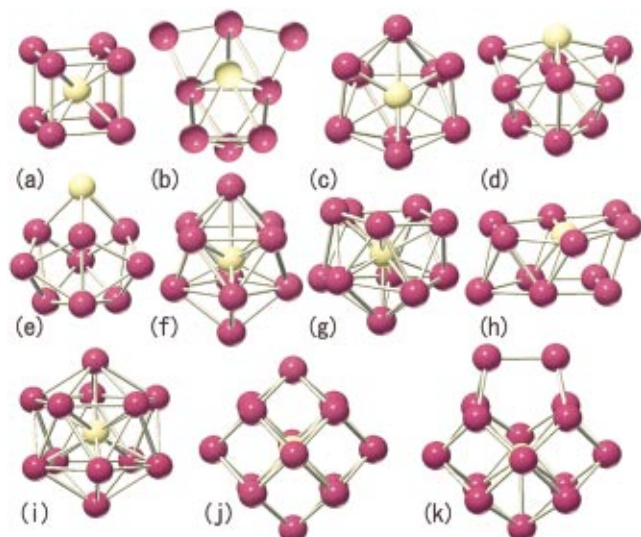


FIG. 1. (Color) M -doped MX_N clusters: (a) c - $M@X_8$, (b) PBP- MX_8 , (c) MX_9 with M inside, (d) MX_9 with M outside close to the triangle of X , (e) MX_9 with M far from the triangle, (f) MX_{10} , (g) i - MX_{11} , (h) ha - MX_{11} , (i) $M@X_{12}$, (j) c - $M@X_{14}$, and (k) c - $M@X_{15}$.

The interaction energy of the magic cluster Si_{10} with Be is significant and it could be much stronger with a transition M atom as found for other clusters.¹ The second order difference in energy shows Si_9 Be to be magic. Adding a Si atom leads to Si_{11} Be that has i structure with a Si atom missing [Fig. 1(g)]. It lies 0.70 eV lower in energy than the one [Fig. 1(h)] derived from a hexagonal antiprism (ha). However, the gap is small (0.57 eV) and the gain in energy in going from Be@ Si_{10} to Si_{11} Be, only 2.44 eV making Si_{11} Be unlikely to be abundant. Similar results are obtained for Ge clusters. Be doping results in magic behavior of Ge_9 Be with DE=4.28 eV and a large HOMO–LUMO gap of 2.16 eV. More interestingly doping of Ge_{10} [Fig. 1(f)] leads to a large gain (4.19 eV) as well as an increase in the gap from 1.94 to 2.0 eV. Also Be@ Sn_{10} shows a gain of 4.08 eV and a large

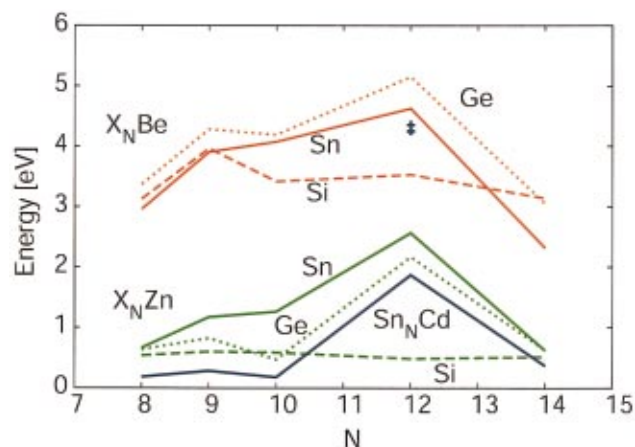


FIG. 2. (Color) Doping energy of M atom in X_N clusters. The crosses correspond to Mn doping in Ge and Sn. The lines are drawn to aid eyes.

gap of 1.85 eV. Therefore, the elemental magic clusters X_{10} become increasingly more stable in going from $X=Si$ to Sn with Be doping (Fig. 2). Note that there is an increase in the DE in going from $N=9$ to 10 for Sn as compared to a decrease for Si or Ge. Doping with Zn or Cd leads to only a small gain in energy in most cases due to their large size. This makes it more favorable to dope outside the prism but the bonding is again weak because of the closed electronic shell structure of X_{10} and the divalent M atoms.

Be@ Si_{12} was earlier shown⁵ to have a chair shaped structure. Doping of Si_{12} with Zn leads to a threefold symmetric structure similar to the one obtained for an isomer⁵ of Si_{12} Be, to be the lowest in energy. The HOMO–LUMO gap is 1.79 eV. An isomer in which Zn interacts outside Si_{12} lies slightly higher in energy. The DE decreases sharply from 3.53 to 0.49 eV in going from Be to Zn while Cd doping is energetically favorable only outside. Similar studies on Ge and Sn, however, show i isomer [Fig. 1(i)] to be the most stable. The gap for Cd@ Ge_{12} is large (2.17 eV) as also⁵ for

TABLE I. BEs (eV/atom), DEs (eV), and the HOMO–LUMO gaps (eV) of some low energy isomers of M doped X_N clusters.

Cluster	BE	DE	Gap	Cluster	BE	DE	Gap
PBP- Si_8 Be	3.59	3.13	1.41	Si_9 Zn (far)	3.38	0.62	0.78
c -Be@ Si_8	3.58	3.01	2.03	Si_9 Zn (near)	3.38	0.60	1.59
PBP- Ge_8 Be	3.16	3.37	1.28	Ge_9 Zn	2.98	0.83	1.52
c -Be@ Ge_8	3.14	3.22	1.75	Sn_9 Zn	2.68	1.17	1.80
c -Be@ Sn_8	2.79	2.96	1.44	Sn_9 Cd	2.59	0.28	1.21
PBP- Sn_8 Be	2.77	2.84	0.96	Ge_{10} Zn	3.06	0.47	1.91
Si_9 Be	3.72	3.96	1.93	Zn@ Sn_{10}	2.76	1.26	1.64
Ge_9 Be	3.33	4.28	2.16	ha -Zn@ Si_{12}	4.16	0.49	1.79
Sn_9 Be	2.95	3.91	1.66	h -Mn@ Si_{12}	3.87	4.99	1.60
Be@ Si_{10}	3.81	3.42	1.68	i -Mg@ Ge_{12}	3.13	2.08	2.30
Be@ Ge_{10}	3.39	4.19	2.00	i -Zn@ Ge_{12}	3.13	2.17	2.21
Be@ Sn_{10}	3.01	4.08	1.85	i -Mn@ Ge_{12}	3.29	4.25	1.10
i -Be@ Ge_{12}	3.36	5.15	2.25	i -Mg@ Sn_{12}	2.86	3.05	2.00
i -Be@ Sn_{12}	2.98	4.62	1.97	i -Ca@ Sn_{12}	2.81	2.38	1.92
d -Be@ Si_{12}	3.74	3.53	1.32	i -Mn@ Sn_{12}	2.96	4.36	1.15
c -Be@ Si_{14}	3.80	3.14	2.02	i -Zn@ Sn_{12}	2.82	2.57	1.96
c -Be@ Ge_{14}	3.29	3.05	1.86	i -Cd@ Sn_{12}	2.77	1.87	1.94
c -Be@ Sn_{14}	2.87	2.32	1.47	c -Mg@ Ge_{14}	3.14	0.87	1.65
PBP- Ge_8 Zn	2.86	0.64	1.17	Ge_{14} Zn	3.13	0.63	1.68
PBP- Sn_8 Zn	2.53	0.67	0.95	c -Mg@ Sn_{14}	2.81	1.44	1.50
PBP- Sn_8 Cd	2.48	0.19	0.91	c -Zn@ Sn_{14}	2.79	0.62	1.47

Zn@Ge₁₂, but the gain in energy is only 0.57 eV as compared to 2.3 eV for Zn. Cd outside Ge₁₂ is nearly degenerate. On the other hand DE of 5.28 (4.63) eV for Be is the highest and the HOMO–LUMO gap is 2.25 (1.97) eV for Ge (Sn). Such large gaps are likely to make these clusters to be luminescent in the visible range. Also *i*-Zn@Sn₁₂ has the lowest energy and large gap (1.96 eV). These results show *M*@*X*₁₂, *X*=Ge and Sn to be the most striking with perfect *i* symmetry and large gaps (Table I). Be doping is exceptionally stable. We also studied doping with Mg and obtained large gaps of ≈2.0 eV for *i*-Mg@*X*₁₂, *X*=Ge and Sn, but the DE for Ge is small (Table I). The *M*–*X* and *X*–*X* bond lengths increase slightly as the size of the *M* atom increases: Be–Sn=2.98 and Sn–Sn=3.13 Å, Zn–Sn=3.02 and Sn–Sn=3.17 Å, Cd–Sn=3.06 and Sn–Sn=3.22 Å, and Mg–Sn=3.05 and Sn–Sn=3.21 Å. Therefore, the large *M* atoms are quite compressed inside the *X* cages that leads to their lower DEs. We checked further for Ca and in spite of its large size, the Ca–Sn bond is 3.13 Å and the DE significant (Table I) due to some *d* contribution to bonding.

The most interesting finding is the magnetic clusters of Ge and Sn with Mn doping. The doping of *X*₁₂ leads to perfect *i* clusters with 5 μ_B magnetic moment in accordance with the Hund's rule.⁷ The Mn–Ge, Ge–Ge, Mn–Sn, and Sn–Sn bond lengths are 2.68, 2.82, 3.01, and 3.17 Å, respectively. The DE for Ge₁₂ and Sn₁₂ is ≈4.3 eV (Fig. 2 and Table I) and the HOMO–LUMO gap, ≈1.1 eV. These are the first high symmetry superatoms of semiconductors with a large magnetic moment. *h* and *ha* isomers have 1 μ_B magnetic moment and lie, respectively, 0.19 (2.654) and 0.02 (1.979) eV higher in energy for Ge (Sn) whereas a decahedral isomer transforms into the *i* isomer. However, for Mn@Si₁₂, the *h* isomer lies 2.93 eV lower in energy with 1 μ_B magnetic moment than the *i* isomer. It has a large HOMO–LUMO gap of 1.6 eV even with an odd number of electrons. Therefore, it is quite stable and interesting for cluster assembly.

Further studies on *X*₁₄*M* in *c*, *h*, and *ha* (capped hexagonal faces) structures show a perfect body centered *c* isomer to have the lowest energy for several *X* and *M* [Fig. 1(j)]. The BE and gap decrease as one goes down from Si to Sn for *M*=Be (Table I) due to reduced interaction of Be with *X*. Be outside Ge₁₄ is nearly degenerate. The largest gap is for Be@Si₁₄ with a value of 2.02 eV. Further calculations on Be@Si₁₅ by adding a Si atom on one of the faces of Be@Si₁₄ cube converge to a structure shown in Fig. 1(k). The DE is 3.19 eV as compared to the BE of 3.8 eV/atom for Be@Si₁₄ suggesting the latter to be magic. Cation and anion Be@Si₁₄ clusters show minimum changes in the structure as compared to the neutral one and a magnetic moment of 1 μ_B . The adiabatic IP is large (7.01 eV) and the EA, low (2.2 eV), as expected for magic clusters. Doping of Mn in *X*₁₄ leads to a magnetic moment of 1 μ_B (5 μ_B) and a DE of 3.16 eV (2.701 eV) for *X*=Ge (Sn). These results show that for *N*=14, in all cases the DE is lower than the BE of clusters and therefore, the probability of forming such clusters is low. Among all *i*-*M*@*X*₁₂ clusters are most striking with particular stability for *M*=Be.

The stability of *i*-*M*@*X*₁₂ was discussed earlier.⁵ For the high symmetry clusters, *M*@*X*₁₀ and *M*@*X*₁₄ it can be understood from the energy spectra of the undoped (empty center, fixed configuration) and doped clusters. In the *M*@*X*₁₀ structure, the downspin HOMO of *X*₁₀ cage is triply degenerate but it has only one electron. Therefore, doping of a divalent *M* atom completely fills this state and leads to a stable isomer with a large HOMO–LUMO gap. Similarly for *c*-*M*@*X*₁₄, the *X*₁₄ cage has a doubly degenerate downspin unoccupied state followed by a large gap. Again doping with a divalent *M* atom completely fills this state and leads to a large gap and the stability of this cluster. The large magnetic moment with Mn doping is due to the large exchange splitting (3.17 eV) of the 3*d* states and the high symmetry of the clusters. We also calculated the frequency spectra using the Gaussian program¹⁰ for *X*_{*N*}Be, *N*=9, 10, 12, and 14, *X*=Si and Ge as well as for Ge₁₂Mn. In all cases these are found to be positive indicating the stability of these structures. Also the results of the BE and the gap are similar to those obtained by the plane wave method.

In summary, we have studied the effects of divalent *M* atom doping on the stability of small Si, Ge, and Sn clusters. The ten-atom magic clusters of these elements can be made more symmetric and stable by *M* doping while the nonmagic clusters such as *X*₉, *X*₁₂, and *X*₁₄ become magic with large gaps. An *i* isomer of Ge and Sn is specially stable with Be doping while Mn doping leads to a perfect *i* superatom with 5 μ_B magnetic moment for Ge and Sn as well as a magnetic Mn@Si₁₂ cluster with a large HOMO–LUMO gap. We hope that these findings will further stimulate research on *M* encapsulated semiconductor clusters.

The authors are thankful to T.M. Briere for helpful discussions. V.K. thankfully acknowledges the kind hospitality at the Institute for Materials Research and the Center for Interdisciplinary Research, the financial support from JSPS and support of the staff of the Center for Computational Materials Science of IMR-Tohoku University for the use of SR8000/G1-64 supercomputer facilities.

¹V. Kumar and Y. Kawazoe, Phys. Rev. Lett. **87**, 045503 (2001); V. Kumar, C. Majumder, and Y. Kawazoe, Chem. Phys. Lett. **363**, 319 (2002).

²H. Hiura, T. Miyazaki, and T. Kanayama, Phys. Rev. Lett. **86**, 1733 (2001).

³V. Kumar and Y. Kawazoe, Phys. Rev. B **65**, 073404 (2002).

⁴V. Kumar and Y. Kawazoe, Phys. Rev. Lett. **88**, 235504 (2002).

⁵V. Kumar and Y. Kawazoe, Appl. Phys. Lett. **80**, 859 (2002).

⁶K.-M. Ho, A. A. Shvartsburg, B. Pan, Z.-Y. Lu, C.-Z. Wang, J. G. Wacker, J. L. Fye, and M. F. Jarrold, Nature (London) **392**, 582 (1998); L. Mitas, J. C. Grossman, I. Stich, and J. Tobik, Phys. Rev. Lett. **84**, 1479 (2000); A. A. Shvartsburg, B. Liu, Z.-Y. Lu, C.-Z. Wang, M. F. Jarrold, and K. M. Ho, Phys. Rev. Lett. **83**, 2167 (1999); C. Majumder, V. Kumar, H. Mizuseki, and Y. Kawazoe, Phys. Rev. B **64**, 233405 (2001).

⁷V. Kumar and Y. Kawazoe, Phys. Rev. B **64**, 115405 (2001).

⁸G. Kresse and J. Furthmüller, Phys. Rev. B **54**, 11169 (1996); D. Vanderbilt, *ibid.* **41**, 7892 (1990).

⁹J. P. Perdew, in *Electronic Structure of Solids '91*, edited by P. Ziesche and H. Eschrig (Akademie, Berlin, 1991).

¹⁰Gaussian 98, Revision A.11.1, Gaussian Inc., Pittsburgh, PA, 2001.

¹¹Values of the HOMO–LUMO gaps are generally underestimated in GGA and the true values may be about 40% higher.